

Rethinking Vision Transformer and Masked Autoencoder in Multimodal Face Anti-Spoofing

Zitong Yu¹, Rizhao Cai², Yawen Cui³, Xin Liu⁴, Yongjian Hu⁵, Alex Kot²

¹Great Bay University ²Nanyang Technological University ³University of Oulu

⁴Lappeenranta-Lahti University of Technology ⁵South China University of Technology

Abstract

Recently, vision transformer (ViT) based multimodal learning methods have been proposed to improve the robustness of face anti-spoofing (FAS) systems. However, there are still no works to explore the fundamental natures (e.g., modality-aware inputs, suitable multimodal pre-training, and efficient finetuning) in vanilla ViT for multimodal FAS. In this paper, we investigate three key factors (i.e., inputs, pre-training, and finetuning) in ViT for multimodal FAS with RGB, Infrared (IR), and Depth. First, in terms of the ViT inputs, we find that leveraging local feature descriptors benefits the ViT on IR modality but not RGB or Depth modalities. Second, in observation of the inefficiency on direct finetuning the whole or partial ViT, we design an adaptive multimodal adapter (AMA), which can efficiently aggregate local multimodal features while freezing majority of ViT parameters. Finally, in consideration of the task (FAS vs. generic object classification) and modality (multimodal vs. unimodal) gaps, ImageNet pre-trained models might be sub-optimal for the multimodal FAS task. To bridge these gaps, we propose the modality-asymmetric masked autoencoder (M^2A^2E) for multimodal FAS self-supervised pre-training without costly annotated labels. Compared with the previous modality-symmetric autoencoder, the proposed M^2A^2E is able to learn more intrinsic task-aware representation and compatible with modality-agnostic (e.g., unimodal, bimodal, and trimodal) downstream settings. Extensive experiments with both unimodal (RGB, Depth, IR) and multimodal (RGB+Depth, RGB+IR, Depth+IR, RGB+Depth+IR) settings conducted on multimodal FAS benchmarks demonstrate the superior performance of the proposed methods. We hope these findings and solutions can facilitate the future research for ViT-based multimodal FAS.

1. Introduction

Face recognition technology has widely used in many intelligent systems due to their convenience and remarkable accuracy. However, face recognition systems are still vul-

nerable to presentation attacks (PAs) ranging from print, replay and 3D-mask attacks. Therefore, both the academia and industry have recognized the critical role of face anti-spoofing (FAS) for securing the face recognition system.

In the past decade, plenty of hand-crafted features based [6, 7, 23, 37] and deep learning based [2, 12, 13, 31, 38, 45] methods have been proposed for unimodal FAS. Despite satisfactory performance in seen attacks and environments, unimodal methods generalize poorly on emerging novel attacks and unseen deployment conditions. Thanks to the advanced sensors with various modalities (e.g., RGB, Infrared (IR), Depth, Thermal) [17], multimodal methods facilitate the FAS applications under some high-security scenarios with low false acceptance errors (e.g., face payment and vault entrance guard).

Recently, due to the strong long-range and cross-modal representation capacity, vision transformer (ViT) [11] based methods [15, 26] have been proposed to improve the robustness of FAS systems. However, these methods focus on direct finetuning ViTs [15] or modifying ViTs with complex and powerful modules [26], which cannot provide enough insights on bridging the fundamental natures (e.g., modality-aware inputs, suitable multimodal pre-training, and efficient finetuning) of ViT in multimodal FAS. Despite mature exploration and finds [3, 18, 44] of ViT on other computer vision communities (e.g., generic object classification [8]), these knowledge might not be fully aligned for the multimodal FAS due to the task and modality gaps.

Compared with CNN, ViT usually aggregates the coarse intra-patch info at the very early stage and then propagates the inter-patch global attentional features. On other words, it neglects the local detailed clues for each modality. According to the prior evidence from MM-CDCN [48], local fine-grained features from multiples levels benefits the live/spoof clue representation in convolutional neural networks (CNN) from different modalities. *Whether local descriptors/features can improve the ViT-based multimodal FAS systems is worth exploring.*

Compared with CNNs, ViTs usually have huger parameters to train, which easily overfit on the FAS task with lim-

ited data amount and diversity. Existing works show that direct finetuning the last classification head [15] or training extra lightweight adapters [20] can achieve better performance than fully finetuning. However, all these observations are based on the unimodal RGB inputs, it is unclear how different ViT-based transfer learning techniques perform on 1) other unimodal scenario (IR or Depth modality); and 2) multimodal scenario (e.g., RGB+IR+Depth). Moreover, *to design more efficient transfer learning modules for ViT-based multimodal FAS should be considered.*

Existing multimodal FAS works usually finetune the ImageNet pre-trained models, which might be sub-optimal due to the huge task (FAS vs. generic object classification) and modality (multimodal vs. unimodal) gaps. Meanwhile, in consideration of costly collection of large-scale annotated live/spoof data, self-supervised pre-training without labels [34] is potential for model initialization in multimodal FAS. Although a few self-supervised pre-training methods (e.g., masked image modeling (MIM) [3, 9] and contrastive learning [1]) are developed for multimodal (e.g., vision-language) applications, there are still no self-supervised pre-trained models specially for multimodal FAS. *To investigate the discrimination and generalization capacity of pre-trained models and design advanced self-supervision strategies are crucial for ViT-based multimodal FAS.*

Motivated by the discussions above, in this paper we rethink the ViT-based multimodal FAS into three aspects, i.e., modality-aware inputs, suitable multimodal pre-training, and efficient finetuning. Besides the elaborate investigations, we also provide corresponding elegant solutions to 1) establish powerful inputs with local descriptors [5, 10] for IR modality; 2) efficiently finetune multimodal ViTs via adaptive multimodal adapters; and 3) pre-train generalized multimodal model via modality-asymmetric masked autoencoder. Our contributions include:

- We are the first to investigate three key factors (i.e., inputs, pretraining, and finetuning) for ViT-based multimodal FAS. We find that 1) leveraging local feature descriptors benefits the ViT on IR modality; 2) partially finetuning or using adapters can achieve reasonable performance for ViT-based multimodal FAS but still far from satisfaction; and 3) mask autoencoder [3, 18] pre-training cannot provide better finetuning performance compared with ImageNet pre-trained models.
- We design the adaptive multimodal adapter (AMA) for ViT-based multimodal FAS, which can efficiently aggregate local multimodal features while freezing majority of ViT parameters.
- We propose the modality-asymmetric masked autoencoder (M²A²E) for multimodal FAS self-supervised pre-training. Compared with modality-symmetric autoencoders [3, 18], the proposed M²A²E is able to learn

more intrinsic task-aware representation and compatible with modality-agnostic downstream settings. To our best knowledge, this is the first attempt to design the MIM framework for generalized multimodal FAS.

- Our proposed methods achieve state-of-the-art performance with most of the modality settings on both intra- as well as cross-dataset testings.

2. Related Work

Multimodal face anti-spoofing. With multimodal inputs (e.g., RGB, IR, Depth, and Thermal), there are a few multimodal FAS works that consider input-level [14, 30, 35, 35] and decision-level [54] fusions. Besides, mainstream FAS methods extract complementary multi-modal features using feature-level fusion [25, 26, 28, 41, 48, 56] strategies. As there are redundancy across multi-modal features, direct feature concatenation [48] easily results in high-dimensional features and overfitting. To alleviate this issue, Zhang et al. [55, 56] propose a feature re-weighting mechanism to select the informative and discard the redundant channel features among RGB, IR, and Depth modalities. Shen et al. [39] design a Modal Feature Erasing operation to randomly dropout partial-modal features to prevent modality-aware overfitting. George and Marcel [16] present a cross-modal focal loss to modulate the loss contribution of each modality, which benefits the model to learn complementary information among modalities.

Transformer for vision tasks. Transformer is proposed in [40] to model sequential data in the field of NLP. Then ViT [11] is proposed recently by feeding transformer with sequences of image patches for image classification. In consideration of the data hungry characteristic of ViT, direct training ViTs from scratch would result in severe overfitting. On the one hand, fast transferring (e.g., adapter [8, 19, 22] and prompt [57] tuning) while fixed most of pre-trained models' parameters is usually efficient for downstream tasks. On the other hand, self-supervised masked image modeling (MIM) methods (e.g., BEiT [4] and MAE [3, 18]) benefit the excellent representation learning, which improve the finetuning performance in downstream tasks.

Meanwhile, a few works introduce vision transformer for FAS [15, 26, 33, 42, 43, 47]. On the one hand, ViT is adopted in the spatial domain [15, 33, 42] to explore live/spoof relations among local patches. On the other hand, global features temporal abnormality [43] or physiological periodicity [47] are extracted applying ViT in the temporal domain. Recently, Liu and Liang [26] develop the modality-agnostic transformer blocks to supplement liveness features for multimodal FAS. Despite convincing performance via modified ViT with complex customized modal-disentangled and cross-modal attention modules [26], there are still no works to explore the fundamental natures (e.g., modality-

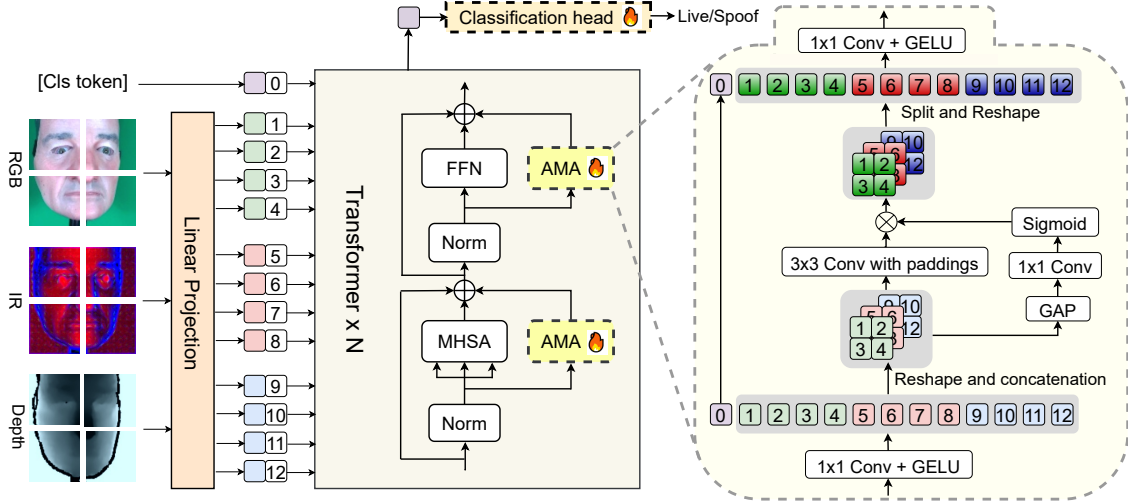


Figure 1. Framework of the ViT finetuning with adaptive multimodal adapters (AMA). The AMA and classification head are **trainable** while the linear projection and vanilla transformer blocks are fixed with the pre-trained parameters. ‘MHSA’, ‘FFN’, and ‘GAP’ are short for the multihead self-attention, feed-forward network, and global average pooling, respectively.

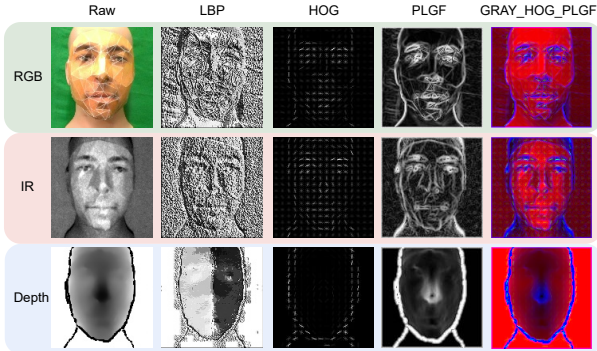


Figure 2. Visualization of three classical local descriptors (i.e., LBP [36], HOG [10], and PLGF [5]) and their compositions.

aware inputs, suitable multimodal pre-training, and efficient finetuning in vanilla ViT for multimodal FAS.

3. Methodology

To benefit the exploration of fundamental natures of ViT for multimodal FAS, here we adopt the *simple, elegant, and unified* ViT framework as baselines. As illustrated in the left part (without ‘AMA’) of Fig. 1, the vanilla ViT consists of a patch tokenizer $\mathbf{E}_{\text{patch}}$ via linear projection, N transformer blocks $\mathbf{E}_{\text{trans}}^i$ ($i = 1, \dots, N$) and a classification head \mathbf{E}_{head} . The unimodal ($X_{\text{RGB}}, X_{\text{IR}}, X_{\text{Depth}}$) or multimodal ($X_{\text{RGB+IR}}, X_{\text{RGB+Depth}}, X_{\text{IR+Depth}}, X_{\text{RGB+IR+Depth}}$) inputs are passed over $\mathbf{E}_{\text{patch}}$ to generate the visual tokens T^{Vis} , which is concatenated with learnable class token T^{Cls} , and added with position embeddings. Then all patch tokens $T^{\text{All}} = [T^{\text{Vis}}, T^{\text{Cls}}]$ will be forwarded with $\mathbf{E}_{\text{trans}}$. Finally, T^{Cls} is sent to \mathbf{E}_{head} for binary live/spoof classification.

We will first briefly introduce different local descriptor based inputs in Sec. 3.1, then introduce the efficient ViT finetuning with AMA in Sec. 3.2, and at last present the generalized multimodal pre-training via M²A²E in Sec. 3.3.

3.1. Local Descriptors for Multimodal ViT

Besides the raw multimodal inputs, we consider three local features and their compositions for multimodal ViT. The motivations behind are that the vanilla ViT with raw inputs is able to model rich cross-patch semantic contexts but sensitive to illumination and neglecting the local fine-grained spoof clues. Explicitly leveraging local descriptors as inputs might benefit multimodal ViT mining more discriminative fine-grained spoof clues [46, 48, 49, 51] as well as illumination-robust live/spoof features [25].

Local binary pattern (LBP). LBP [36] computes a binary pattern via thresholding central difference among neighborhood pixels. Fine-grained textures and illumination invariance make LBP robust for generalized FAS [24]. For a center pixel I_c and a neighboring pixel I_i ($i = 1, 2, \dots, p$), LBP can be formalized as follows:

$$\text{LBP} = \sum_{i=1}^p F(I_i - I_c) \times 2^{i-1}, \quad (1)$$

$$F(I) = \begin{cases} 1, & I \geq 0, \\ 0, & \text{otherwise.} \end{cases}$$

Typical LBP maps are shown in second column of Fig. 2.

Histograms of oriented gradients (HOG). HOG [10] describes the distribution of gradient orientations or edge directions within a local subregion. It is implemented via firstly computing magnitudes and orientations of gradients at each pixel, and then the gradients within each small local subregion are accumulated into orientation histogram vectors of several bins, voted by gradient magnitudes. Due to the partial invariance to geometric and photometric changes, HOG features might be robust for the illumination-sensitive modalities like RGB and IR. The visualization results are shown in third column of Fig. 2.

Pattern of local gravitational force (PLGF). Inspired by Law of Universal Gravitation, PLGF [5] describes the image interest regions via local gravitational force magnitude, which is useful to reduce the impact of illumination/noise variation while preserving edge-based low-level clues. It can be formulated as:

$$\begin{aligned}
 \text{PLGF} &= \arctan\left(\sqrt{\left(\frac{I * M_x}{I}\right)^2 + \left(\frac{I * M_y}{I}\right)^2}\right), \\
 M_x(m, n) &= \begin{cases} \frac{\cos(\arctan(m/n))}{m^2+n^2}, & (m^2 + n^2) > 0, \\ 0, & \text{otherwise,} \end{cases} \quad (2) \\
 M_y(m, n) &= \begin{cases} \frac{\sin(\arctan(m/n))}{m^2+n^2}, & (m^2 + n^2) > 0, \\ 0, & \text{otherwise,} \end{cases}
 \end{aligned}$$

where I is the raw image. M_x and M_y are two filter masks for gravitational force calculation. m and n are indexes denoting the relative position to the center. $*$ is convolution operation sliding along all pixels. The visualization of PLGF maps are shown in fourth column of Fig. 2.

Composition. In consideration of the complementary characteristics from raw image and local descriptors, we also study the compositions among these features via input-level concatenation. For example, ‘GRAY_HOG_PLFG’ denotes three-channel inputs (raw gray-scale channel + HOG + PLFG), which is visualized in last column of Fig. 2.

3.2. Adaptive Multimodal Adapter

Recent studies have verified that introducing adapters [20] with fully connected (FC) layers can improve the FAS performance when training data is not adequate. However, FC-based adapter focuses on the intra-token feature refinement but neglects 1) contextual features from local neighbor tokens; and 2) multimodal features from cross-modal tokens. To tackle these issues, we extend the convolutional adapter (ConvAdapter) [22] into a multimodal version for multimodal FAS.

As illustrated in Fig. 1, instead of directly finetuning the transformer blocks $\mathbf{E}_{\text{trans}}$, we fix all the pre-trained parameters from $\mathbf{E}_{\text{patch}}$ and $\mathbf{E}_{\text{trans}}$ while training only adaptive multimodal adapters (AMA) and \mathbf{E}_{head} . An AMA module consists of four parts: 1) an 1×1 convolution with GELU Θ_{\downarrow} for dimension reduction from the original channels D to a hidden dimension D' ; 2) a 3×3 2D convolution Θ_{2D} mapping channels $D' \times K$ to D' for multimodal local feature aggregation, where K means the modality numbers; 3) an adaptive modality weight (w_1, \dots, w_K) generator via cascading global averaging pooling (GAP), 1×1 convolution Θ_{Ada} to project channels from $D' \times K$ to K , and the Sigmoid function σ ; and 4) an 1×1 convolution with GELU Θ_{\uparrow} for dimension expansion to D . As features from different modalities are already spatially aligned, we restore the 2D structure for each modality after the channel squeezing. Similarly, the 2D structure will be flattened into 1D tokens before

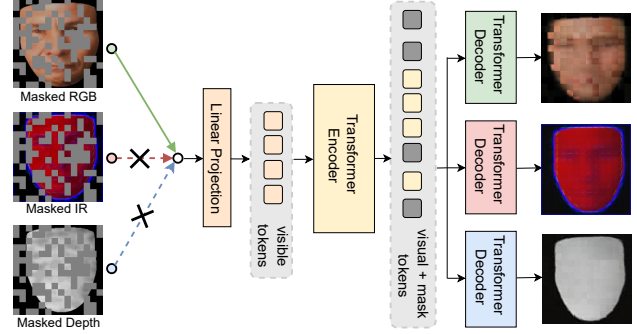


Figure 3. The framework of the modality-asymmetric masked autoencoder (M^2A^2E). Different from previous multimodal MAE [3] masking all modalities as inputs, our M^2A^2E randomly selects unimodal masked input for multimodal reconstruction.

the channel expanding. The AMA can be formulated as

$$\begin{aligned}
 T_{\text{Kmodal}}^{\text{Vis}} &= \text{Concat}[\Theta_{\downarrow}(T_{\text{RGB}}^{\text{Vis}}), \Theta_{\downarrow}(T_{\text{IR}}^{\text{Vis}}), \Theta_{\downarrow}(T_{\text{Depth}}^{\text{Vis}})], \\
 w_{\text{RGB}}, w_{\text{IR}}, w_{\text{Depth}} &= \sigma(\Theta_{\text{Ada}}(\text{GAP}(T_{\text{Kmodal}}^{\text{Vis}}))), \\
 T_{\text{Kmodal}}^{\text{Vis}} &= \Theta_{2D}(T_{\text{Kmodal}}^{\text{Vis}}), \\
 T_{\text{Kmodal}}^{\text{Vis}} &= \text{Concat}[w_{\text{RGB}} \cdot T_{\text{Kmodal}}^{\text{Vis}}, w_{\text{IR}} \cdot T_{\text{Kmodal}}^{\text{Vis}}, w_{\text{Depth}} \cdot T_{\text{Kmodal}}^{\text{Vis}}], \\
 \text{AMA} &= \text{Concat}[\Theta_{\uparrow}(\Theta_{\downarrow}(T^{\text{Cls}})), \Theta_{\uparrow}(T_{\text{Kmodal}}^{\text{Vis}})]. \quad (3)
 \end{aligned}$$

Here we show an example when $K=3$ (i.e., RGB+IR+Depth) in Eq.(3), and AMA is flexible for arbitrary modalities (e.g., RGB+IR). Note that AMA is equivalent to vanilla ConvAdapter [22] in unimodal setting when $K=1$.

3.3. Modality-Asymmetric Masked Autoencoder

Existing multimodal FAS works usually finetune the ImageNet pre-trained models, which might be sub-optimal due to the huge task and modality gaps. Meanwhile, in consideration of costly collection of large-scale annotated live/spoof data, self-supervised pre-training without labels [34] is potential for model initialization in multimodal FAS. Here we propose the modality-asymmetric masked autoencoder (M^2A^2E) for multimodal FAS self-supervised pre-training.

As shown in Fig. 8, given a multimodal face sample $(X_{\text{RGB}}, X_{\text{IR}}, X_{\text{Depth}})$, M^2A^2E randomly selects unimodal input X_i ($i \in \text{RGB, IR, Depth}$) among all modalities. Then random sampling strategy [18] is used to mask out p percentage of the visual tokens in X_i . Only the unmasked visible tokens are forwarded the ViT encoder and both visible and masked tokens are fed in unshared ViT decoders. In terms of the reconstruction target, given a masked input X_i with the i -th modality, M^2A^2E aims to predict the pixel values with mean squared error (MSE) loss for 1) each masked patch of X_i , and 2) the whole input images of other modalities X_j ($j \neq i; j \in \text{RGB, IR, Depth}$). The motivation behind M^2A^2E is that with the multimodal reconstruction target, the self-supervised pre-trained ViTs are able to model

Table 1. ACER(%) results of protocols ‘seen’ and ‘unseen’ on WMCA. The values ACER(%) reported on testing sets are obtained with thresholds computed for BPCER=1% on development sets. Best results are marked in **bold**. ‘ConvA’ indicates the ConvAdapter [22].

Method	Seen	Unseen							
		Flexiblemask	Replay	Fakehead	Prints	Glasses	Papermask	Rigidmask	mean±std
Modality: RGB									
MC-CNN [17]	32.82	22.80	31.40	1.90	30.00	50.00	4.80	18.30	22.74±15.33
CCL(ResNet50) [29]	30.69	4.76	15.37	24.67	19.03	16.80	9.51	17.62	15.39±6.51
CCL(CDCN) [29]	27.14	7.18	11.79	21.82	20.53	35.13	18.91	15.10	18.64±8.91
ViT [11]	9.84	18.4	19.94	13.67	1.92	24.58	5.59	9.59	13.38+8.17
ViT+ConvA (Ours)	4.72	18.64	10.07	7.98	0.43	20.14	6.38	2.32	9.42+7.56
ViT+ConvA+M²A²E (Ours)	8.95	23.68	11.42	2.28	0.29	27.98	7.20	7.65	11.5+10.52
Modality: IR									
RDWT-Haralick [17]	6.26	-	-	-	-	-	-	-	-
MC-CNN [17]	2.51	-	-	-	-	-	-	-	-
ViT [11]	7.74	14.96	1.85	2.57	0.00	45.63	1.19	1.98	9.74+16.61
ViT+ConvA (Ours)	4.35	9.67	0.00	1.30	0.51	45.63	0.70	0.43	8.32+16.80
ViT+ConvA+M²A²E (Ours)	3.34	13.24	0.14	5.12	0.29	31.24	0.61	0.00	7.23+11.63
Modality: Depth									
MC-CNN [17]	6.04	-	-	-	-	-	-	-	-
ViT [11]	7.78	21.04	0.14	2.86	0.87	37.92	1.05	9.06	10.42+14.22
ViT+ConvA (Ours)	5.73	26.33	0.29	2.57	0.29	36.73	0.94	6.25	10.49+14.83
ViT+ConvA+M²A²E (Ours)	5.31	20.27	0.00	2.57	0.00	36.55	0.43	7.31	9.59+13.92
Modality: RGB+IR									
MA-Net [28]	6.85	25.33	3.16	2.05	0.28	36.72	0.86	9.82	11.18±14.30
ViT [11]	4.02	15.76	19.15	6.42	1.45	23.25	2.19	3.44	10.23+8.96
ViT+AMA (Ours)	1.27	15.49	1.16	1.74	0.43	28.16	1.01	0.77	6.97+11.09
ViT+AMA+M²A²E (Ours)	1.35	8.63	0.29	0.43	0.00	29.47	2.75	0.97	6.08+10.75
Modality: RGB+Depth									
MC-PixBiS [13]	1.80	49.70	3.70	0.70	0.10	16.00	0.20	3.40	10.50±16.70
CMFL [16]	1.70	12.40	1.00	2.50	0.70	33.50	1.80	1.70	7.60±11.20
MA-ViT [26]	1.45	9.76	0.93	0.55	0.00	14.00	0.00	1.46	3.81±5.67
ViT [11]	3.10	18.67	8.87	5.00	0.72	22.52	0.58	3.93	8.61+8.72
ViT+AMA (Ours)	1.19	18.67	1.01	2.03	0.00	16.88	1.16	0.72	5.78+8.23
ViT+AMA+M²A²E (Ours)	2.53	14.45	0.29	0.00	0.00	19.91	3.91	2.19	5.82+8.04
Modality: IR+Depth									
ViT [11]	5.47	15.64	0.00	1.71	0.00	41.03	0.67	2.38	8.78+15.26
ViT+AMA (Ours)	1.88	10.45	0.00	3.92	0.00	41	0.38	1.55	8.19+14.94
ViT+AMA+M²A²E (Ours)	1.96	11.51	0.00	0.98	0.00	34.06	0.00	0.00	6.65+12.81
Modality: RGB+IR+Depth (* indicates with RGB+IR+Depth+Thermal modalities)									
IQM+LBP* [17]	7.54	28.58	0.84	2.38	2.3	50.86	16.34	14.27	16.29±18.36
MC-CNN* [17]	1.04	2.52	0.12	0.00	0.00	42.14	0.35	0.75	6.55±15.72
ViT [11]	2.52	15.88	5.46	0.58	0.14	19.99	0.90	2.32	6.46+8.12
ViT+AMA (Ours)	0.92	15.39	0.64	1.99	0.87	18.37	0.87	0.77	5.56+7.80
ViT+AMA+M²A²E (Ours)	1.39	9.02	0.00	0.00	0.00	17.99	0.00	0.00	3.86+7.08

1) task-aware contextual semantics (e.g., moiré patterns and color distortion) via masked patch prediction; and 2) intrinsic physical features (e.g., 2D attacks without facial depth) via cross modality translation.

Relation to modality-symmetric autoencoders [3, 18]. Compared with the vanilla MAE [18], M²A²E adopts the same masked strategy in unimodal ViT encoder but targeting at multimodal reconstruction with multiple unshared ViT decoders. Besides, M²A²E is similar to the multimodal MAE [3] only when partial tokens from a single modality are visible while masking all tokens from other modalities.

4. Experimental Evaluation

4.1. Datasets and Performance Metrics

Three commonly used multimodal FAS datasets are used for experiments, including WMCA [17], CASIA-SURF (MmFA) [56] and CASIA-SURF CeFA (CeFA) [27]. WMCA contains a wide variety of 2D and 3D PAs with

four modalities, which introduces 2 protocols: ‘seen’ protocol which emulates the seen attack scenario and the ‘unseen’ attack protocol that evaluates the generalization on an unseen attack. **MmFA** consists of 1000 subjects with 21000 videos, and each sample has 3 modalities, which has an official intra-testing protocol. **CeFA** is the largest multimodal FAS dataset, covering 3 ethnicities, 3 modalities, 1607 subjects, and 34200 videos. We conduct intra- and cross-dataset testings on WMCA and MmFA datasets, and leave large-scale CeFA for self-supervised pre-training.

In terms of evaluation metrics, Attack Presentation Classification Error Rate (APCER), Bonafide Presentation Classification Error Rate (BPCER), and ACER [21] are used for the metrics. The ACER on testing set is determined by the Equal Error Rate (EER) threshold on dev sets for MmFA, and the BPCER=1% threshold for WMCA. True Positive Rate (TPR)@False Positive Rate (FPR)=10⁻⁴ [56] is also provided for MmFA. For cross-testing experiments, Half Total Error Rate (HTER) is adopted.

4.2. Implementation Details

We crop the face frames using MTCNN [53] face detector. The local descriptors are extracted from gray-scale images with: 1) 3x3 neighbors for LBP [36]; 2) 9 orientations, 8x8 pixels per cell, and 2x2 cells per block for HOG [10]; and 3) the size of masks are set to 5 for PLGF [5]. Composition inputs ‘GRAY_HOG_PLGF’ are adopted on unimodal and multimodal experiments for IR modality, while the raw inputs are utilized for RGB and Depth modalities. ViT-Base [11] supervised by binary cross-entropy loss is used as the defaulted architecture. For the direct finetuning, only the last transformer block and classification head are trainable. For AMA and ConvAdapter [22] finetuning, the original and hidden channels are $D=768$ and $D'=64$, respectively. For M^2A^2E , the mask ratio $p=40\%$ is used while decoder depth and width is 4 and 512, respectively.

The experiments are implemented with Pytorch on one NVIDIA A100 GPU. For the self-supervised pre-training on CeFA with RGB+IR+Depth modalities, we use the AdamW [32] optimizer with learning rate (lr) $1.5e-4$, weight decay (wd) 0.05 and batch size 64 at the training stage. ImageNet pre-trained weights are used for our encoder. We train the M^2A^2E for 400 epochs while warming up the first 40 epochs, and then performing cosine decay. For supervised unimodal and multimodal experiments on WMCA and MmFA, we use the Adam optimizer with the fixed $lr=2e-4$, $wd=5e-3$ and batch size 16 at the training stage. We finetune models with maximum 30 epochs based on the ImageNet or M^2A^2E pre-trained weights.

4.3. Intra-dataset Testing

Intra testing on WMCA. The unimodal and multimodal results of protocols ‘seen’ and ‘unseen’ on WMCA [17] are shown in Table 1. On the one hand, compared with the direct finetuning results from ‘ViT’, the ViT+AMA/ConvAdapter can achieve significantly lower ACER in all modalities settings and both ‘seen’ and ‘unseen’ protocols. This indicates the proposed AMA efficiently leverages the unimodal/multimodal local inductive cues to boost original ViT’s global contextual features. On the other hand, when replaced the ImageNet pre-trained ViT with self-supervised M^2A^2E from CeFA, the generalization for unseen attack detection improves obviously with modalities ‘IR’, ‘Depth’, ‘RGB+IR’, ‘IR+Depth’, and ‘RGB+IR+Depth’, indicating its excellent transferability for downstream modality-agnostic tasks. It is surprising to find in the last block that the proposed methods with RGB+IR+Depth modalities perform even better than ‘MC-CNN’ [17] with four modalities in both ‘seen’ and ‘unseen’ protocols. With complex and specialized modules, although ‘MA-ViT’ [26] outperforms the proposed methods with RGB+Depth modalities in ‘unseen’ protocol by -2.01% ACER, the proposed AMA and M^2A^2E might be

Table 2. The results on MmFA. Larger TPR and lower ACER values indicate better performance. Best results are marked in **bold**.

Method	APCER(%)	BPCER(%)	ACER(%)	TPR(%) @FPR=10 ⁻⁴
Modality: RGB				
SEF [56]	8.0	14.5	11.3	6.8
MS-SEF [55]	40.3	1.6	21.0	14.6
ViT [11]	18.91	15.83	17.37	16.72
ViT+ConvA (Ours)	10.70	9.33	10.02	20.22
ViT+ConvA+M ² A ² E (Ours)	6.62	6.17	6.40	23.77
Modality: IR				
SEF [56]	15.0	1.2	8.1	10.9
MS-SEF [55]	38.6	0.4	19.4	15.9
ViT [11]	18.74	19.11	18.92	10.72
ViT+ConvA (Ours)	16.30	13.00	14.65	17.36
ViT+ConvA+M ² A ² E (Ours)	12.73	11.44	12.09	19.94
Modality: Depth				
SEF [56]	5.1	4.8	5.0	14.1
MS-SEF [55]	6.0	1.2	3.6	67.3
ViT [11]	2.67	2.22	2.44	36.56
ViT+ConvA (Ours)	1.19	2.61	1.90	64.11
ViT+ConvA+M ² A ² E (Ours)	1.68	2.61	2.15	51.39
Modality: RGB+IR				
SEF [56]	14.4	1.6	8.0	26.1
MS-SEF [55]	36.5	0.005	18.3	37.0
ViT [11]	17.18	18.94	18.06	24.67
ViT+AMA (Ours)	16.83	11.87	14.35	36.67
ViT+AMA+M ² A ² E (Ours)	11.38	11.44	11.41	40.94
Modality: RGB+Depth				
SEF [56]	4.3	5.6	5.0	10.6
MS-SEF [55]	5.8	0.8	3.3	71.1
ViT [11]	5.13	4.06	4.60	36.22
ViT+AMA (Ours)	1.29	2.39	1.84	67.89
ViT+AMA+M ² A ² E (Ours)	1.25	2.06	1.65	75.06
Modality: IR+Depth				
SEF [56]	1.5	8.4	4.9	24.3
MS-SEF [55]	2.0	0.3	1.1	81.2
ViT [11]	2.08	3.28	2.68	40.39
ViT+AMA (Ours)	1.56	1.78	1.67	59.72
ViT+AMA+M ² A ² E (Ours)	1.48	0.83	1.16	67.33
Modality: RGB+IR+Depth				
SEF [56]	3.8	1.0	2.4	56.8
MS-SEF [55]	1.9	0.1	1.0	92.4
MA-ViT [26]	0.78	0.83	0.80	82.83
ViT [11]	2.10	1.78	1.94	66.61
ViT+AMA (Ours)	2.22	0.49	1.36	78.94
ViT+AMA+M ² A ² E (Ours)	0.81	0.42	0.62	85.23

potential to plug-and-play in ‘MA-ViT’ for further performance improvement.

Intra testing on MmFA. For MmFA, we compare with three famous multimodal methods ‘SEF’ [56], ‘MS-SEF’ [55], and ‘MA-ViT’ [26]. From Table 2, we can observe that the performance of ‘ViT’ is usually worse than ‘MS-SEF’ with multimodal settings due to the limited modality fusion ability. When equipped with AMA and M^2A^2E -based self-supervised pre-training, ‘ViT+AMA+M²A²E’ outperforms MS-SEF by a large margin in most modality settings (‘RGB’, ‘Depth’, ‘RGB+IR’, ‘RGB+Depth’, ‘RGB+IR+Depth’) in terms of ACER metrics. Thanks to the powerful multimodal representation capacity from the M^2A^2E pre-trained model, the proposed method surpasses the dedicated ‘MA-ViT’ with ‘RGB+IR+Depth’ modalities.

4.4. Cross-dataset Testing

To evaluate the unimodal and multimodal generalization, we conduct cross-testing experiments between models trained on MmFA and WMCA with Protocol ‘seen’. We also introduce the ‘MM-CDCN’ [48] and ‘MA-ViT’ [26]

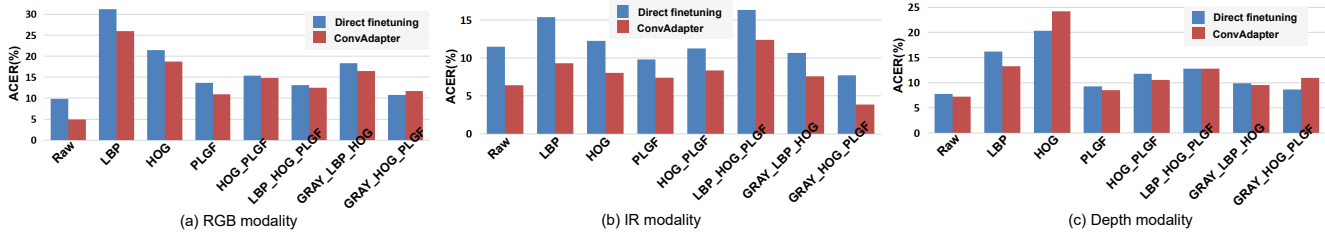


Figure 4. Impacts of inputs with local feature descriptors (e.g., LBP, HOG, PLGF) for ViT using direct finetuning and ConvAdapter strategies on (a) RGB, (b) IR, and (c) Depth modalities. More results on multimodal settings can be found in Appendix A.

Table 3. The HTER (%) values from the cross-testing between WMCA and MmFA datasets. Best results are marked in **bold**.

Method	Train on WMCA Test on MmFA	Train on MmFA Test on WMCA
Modality: RGB		
CDCN [51]	27.47	34.66
ViT [11]	25.18	50.26
ViT+ConvA (Ours)	21.31	35.29
ViT+ConvA+M²A²E (Ours)	23.56	35.69
Modality: IR		
CDCN [51]	44.11	31.19
ViT [11]	35.22	37.88
ViT+ConvA (Ours)	30.61	31.78
ViT+ConvA+M²A²E (Ours)	26.06	26.50
Modality: Depth		
CDCN [51]	31.16	32.11
ViT [11]	27.94	29.53
ViT+ConvA (Ours)	25.04	26.75
ViT+ConvA+M²A²E (Ours)	23.12	23.71
Modality: RGB+IR		
MM-CDCN [48]	24.60	27.86
ViT [11]	27.07	30.63
ViT+AMA (Ours)	19.77	27.80
ViT+AMA+M²A²E (Ours)	17.82	25.67
Modality: RGB+Depth		
MM-CDCN [48]	22.38	25.46
ViT [11]	23.72	29.95
ViT+AMA (Ours)	19.17	24.99
ViT+AMA+M²A²E (Ours)	18.34	25.82
Modality: IR+Depth		
MM-CDCN [48]	29.5	30.22
ViT [11]	31.84	34.99
ViT+AMA (Ours)	25.49	28.04
ViT+AMA+M²A²E (Ours)	21.43	26.35
Modality: RGB+IR+Depth		
Aux.(Depth) [31]	12.35	24.54
MM-CDCN [48]	21.25	21.83
MA-ViT [26]	10.41	20.63
ViT [11]	19.19	23.21
ViT+AMA (Ours)	13.99	20.22
ViT+AMA+M²A²E (Ours)	8.60	18.83

as baselines. Table 3 lists the HTER of all methods trained on one dataset and tested on another dataset. From these results, the proposed ‘ViT+AMA+M²A²E’ outperforms ‘MM-CDCN’ in most modality settings and ‘MA-ViT’ with ‘RGB+IR+Depth’ on both two cross-testing protocols, indicating that the learned multimodal features are robust to the sensors, resolutions, and attack types. Specifically, directly finetuning ImageNet pre-trained ViTs (see results of ‘ViT’) usually generalize worse than ‘MM-CDCN’ in multimodal settings. When assembling with AMA and M²A²E, the HTER can be further reduced 9.25%/5.38%/10.41%/10.59% and 4.96%/4.13%/8.64%/4.38% for ‘RGB+IR’/‘RGB+Depth’/‘IR+Depth’/‘RGB+IR+Depth’ when tested on MmFA and

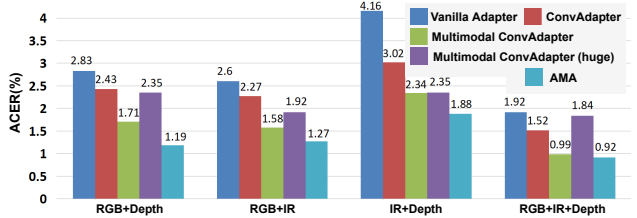


Figure 5. Ablation of the adapter types in transformer blocks.

WMCA, respectively.

4.5. Ablation Study

We also provide the results of ablation studies for inputs with local descriptors and AMA on ‘seen’ protocol of WMCA while studies for M²A²E on ‘unseen’ protocol of WMCA and cross testing from WMCA to MmFA.

Impact of inputs with local descriptors. In the default setting of ViT inputs, composition input ‘GRAY_HOG.PLGF’ is adopted on for IR modality, while the raw inputs are utilized for RGB and Depth modalities. In this ablation, we consider three local descriptors (‘LBP’ [36], ‘HOG’ [10], ‘PLGF’ [5]) and their compositions (‘HOG.PLGF’, ‘LBP.HOG.PLGF’, ‘GRAY_HOG.PLGF’). It can be seen from Fig. 4 that the ‘LBP’ input usually performs worse than other features for all three modalities. In contrast, the ‘PLGF’ input achieves reasonable performance (even better performance than raw input for IR modality via direct finetuning). It is clear that raw inputs are good enough for all modalities via ConvAdapter. One highlight is that composition input ‘GRAY_HOG.PLGF’ performs the best for IR modality via both direct finetuning and ConvAdapter, indicating the importance of local detailed and illumination invariant cues in IR feature representation.

Impact of adapter types. Here we discuss five possible adapter types for efficient multimodal learning, including FC-based ‘vanilla adapter’ [20], independent-modal ‘ConvAdapter’ [22], ‘multimodal ConvAdapter’ with Θ_{2D} mapping channels $D' \times K$ to D' , ‘multimodal ConvAdapter (huge)’ with Θ_{2D} mapping channels $D' \times K$ to $D' \times K$, and adaptive multimodal ConvAdapter (‘AMA’). As shown in Fig. 5, the ConvAdapter based modules perform significantly better than vanilla adapter in multimodal settings, indicating the local inductive biases benefit the ViT-based FAS. Moreover, compared with ‘ConvAdapter’, ‘multi-

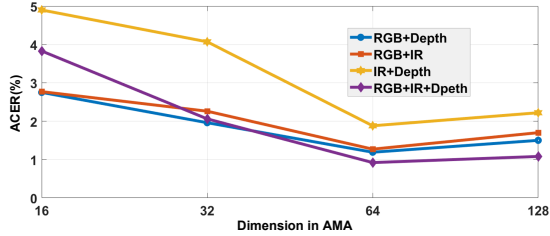


Figure 6. Ablation of the hidden dimensions in AMA.

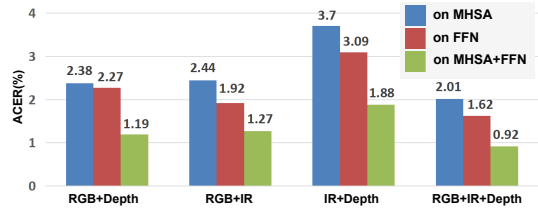


Figure 7. Ablation of the AMA positions in transformer blocks.

modal ConvAdapter’ reduces more than 0.5% ACER in all multimodal settings via aggregating multimodal local features. In contrast, we cannot see any performance improvement from ‘multimodal ConvAdapter (huge)’. In other words, directly learning high-dimensional ($D' \times K$) convolutional features for all K modalities results in serious overfitting. Compared with ‘multimodal ConvAdapter’, AMA enhances the diversity of features for different modalities via adaptively weighting the shared low-dimensional (D') convolutional features, which decreases 0.52%, 0.31%, 1.07%, 0.07% ACER for ‘RGB+Depth’, ‘RGB+IR’, ‘IR+Depth’, ‘RGB+IR+Depth’, respectively.

Impact of dimension and position of AMA. Here we study the hidden dimensions D' in AMA and the impact of AMA positions in transformer blocks. It can be seen from Fig. 6 that despite more lightweight, lower dimensions (16 and 32) cannot achieve satisfactory performance due to weak representation capacity. The best performance can be achieved when $D'=64$ in all multimodal settings. In terms of AMA positions, it is interesting to find from Fig. 7 that plugging AMA along FFN performs better than along MHSA in multimodal settings. This might be because the multimodal local features complement the limitation of point-wise receptive field in FFN. Besides, it is reasonable that applying AMA on MHSA+FFN performs the best.

Impact of mask ratio in M^2A^2E . Fig. 8(a) illustrates the generalization of the M^2A^2E pre-trained ViT when finetuning on ‘unseen’ protocol of WMCA and cross testing from MmFA to WMCA. Different from the conclusions from [3, 18] using very large mask ratio (e.g., 75% and 83%), we find that mask ratio ranges from 30% to 50% are suitable for multimodal FAS, and the best generalization performance on two testing protocols are achieved when mask ratio equals to 40%. In other words, extreme high mask ratios (e.g., 70% to 90%) might force the model to learn too semantic features but ignoring some useful low-/mid-level live/spoof cues.

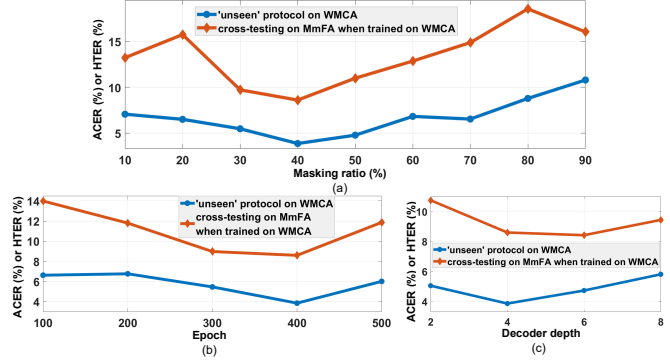


Figure 8. Ablation of the (a) mask ratio; (b) self-supervision training epochs; and (c) decoder depth in M^2A^2E .

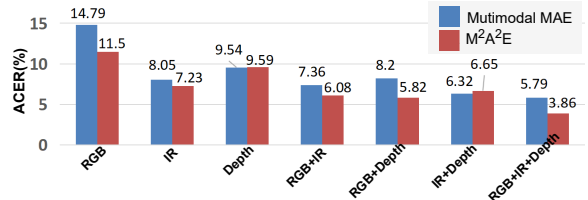


Figure 9. Results of the multimodal MAE [3] and our M^2A^2E .

Impact of training epochs and decoder depth in M^2A^2E .

We also investigate how the training epochs and decoder depth influence the M^2A^2E . As shown in Fig. 8(b) and Fig. 8(c), training M^2A^2E with 400 epochs and decoder of 4 transformer blocks generalizes the best. More training iterations and deeper decoder are not always helpful due to the severe overfits on reconstruction targets.

Comparison between multimodal MAE [3] and M^2A^2E .

We also compare M^2A^2E with the symmetric multimodal MAE [3] when finetuning on all downstream modality settings. It can be seen from Fig. 9 that with more challenging reconstruction target (from masked unimodal inputs to multimodal prediction), M^2A^2E is outperforms the best settings of multimodal MAE [3] on most modalities (‘RGB’, ‘IR’, ‘RGB+IR’, ‘RGB+Depth’, ‘RGB+IR+Depth’), indicating its excellent downstream modality-agnostic capacity.

5. Conclusions and Future Work

In this paper, we investigate three key factors (i.e., inputs, pretraining, and finetuning) for ViT-based multimodal FAS. We propose to combine local feature descriptors for IR inputs, and design the modality-asymmetric masked autoencoder and adaptive multimodal adapter for efficient self-supervised pre-training and supervised finetuning for multimodal FAS. We note that the study of ViT-based multimodal FAS is still at an early stage. Future directions include: 1) Besides inputs, integrating local descriptors into transformer blocks [50] or adapters is potential for ViT-based multimodal FAS; 2) Besides generalization, the discriminative capacity of M^2A^2E pre-trained models should be improved. Some regularization strategies like distillation [52] might be explored.

Appendix A. Ablation on Multimodal Inputs with Local Descriptors

In the default setting of ViT inputs, composition input ‘GRAY_HOG_PLGF’ is adopted on for IR modality, while the raw inputs are utilized for RGB and Depth modalities. Besides the unimodal input results with local descriptors in the main manuscript, we also demonstrate elaborate bimodal and trimodal results with local descriptors on WMCA with Protocol ‘seen’ in Fig. 10 and Fig. 11, respectively. Some observations can be found: 1) in the multimodal settings (RGB+IR, IR+Depth, and RGB+IR+Depth), the composition input ‘GRAY_HOG_PLGF’ for IR modality with raw inputs for other modalities performs the best via both direct finetuning and AMA; and 2) leveraging the local descriptor inputs for IR modality via direct finetuning, the performance on ‘IR+Depth’ and ‘RGB+IR+Depth’ are significantly improved compared with using all raw inputs. They all indicate the importance of local detailed and illumination invariant cues in IR feature representation.

Appendix B. Ablation on Direct Finetuning

Here we discuss five finetuning strategies for ImageNet pretrained ViT-Base including finetuning 1) all transformer blocks and classification head; 2) last 8 transformer blocks and classification head; 3) last 4 transformer blocks and classification head; 4) last transformer block and classification head; and 5) only classification head. The results on WMCA with Protocol ‘seen’ are shown in Fig. 12. The composition input ‘GRAY_HOG_PLGF’ is used for IR modality. It is clear that finetuning all transformer blocks perform the worst due to the overfitting issues in huge trainable parameters. In contrast, finetuning the last transformer block or last 8 transformer blocks can achieve stable and reasonable performance. We adopt the strategy of finetuning last transformer block and classification head as the defaulted direct finetuning setting due to its efficiency.

Appendix C. Visualization of M^2A^2E

We also conduct experiments to visual the reconstruction results of the proposed M^2A^2E . As illustrated in Fig. 13, we find that even though with unimodal (40%) masked input, the reconstruction of all three modalities still keep some important live/spoof clues (e.g., convincing facial geometric depth predicted from masked RGB input for live samples while equivocal depth info for spoof ones), which benefits the self-supervised pre-training for generalized task-aware feature representation.

References

[1] Hassan Akbari, Liangzhe Yuan, Rui Qian, Wei-Hong Chuang, Shih-Fu Chang, Yin Cui, and Boqing Gong. Vatt:

Transformers for multimodal self-supervised learning from raw video, audio and text. *NeurIPS*, 2021.

[2] Yousef Atoum, Yaojie Liu, Amin Jourabloo, and Xiaoming Liu. Face anti-spoofing using patch and depth-based cnns. In *IJCB*, 2017.

[3] Roman Bachmann, David Mizrahi, Andrei Atanov, and Amir Zamir. Multimaec: Multi-modal multi-task masked autoencoders. In *ECCV*, 2022.

[4] Hangbo Bao, Li Dong, and Furu Wei. Beit: Bert pre-training of image transformers. *arXiv preprint arXiv:2106.08254*, 2021.

[5] Debotosh Bhattacharjee and Hiranmoy Roy. Pattern of local gravitational force (plgf): A novel local image descriptor. *IEEE TPMAI*, 2019.

[6] Zinelabidine Boulkenafet, Jukka Komulainen, and Abdenour Hadid. Face anti-spoofing based on color texture analysis. In *ICIP*, 2015.

[7] Zinelabidine Boulkenafet, Jukka Komulainen, and Abdenour Hadid. Face antispoofing using speeded-up robust features and fisher vector encoding. *IEEE SPL*, 24(2):141–145, 2017.

[8] Hao Chen, Ran Tao, Han Zhang, Yidong Wang, Wei Ye, Jindong Wang, Guosheng Hu, and Marios Savvides. Convadapter: Exploring parameter efficient transfer learning for convnets. *arXiv preprint arXiv:2208.07463*, 2022.

[9] Zhihong Chen, Yuhao Du, Jinpeng Hu, Yang Liu, Guanbin Li, Xiang Wan, and Tsung-Hui Chang. Multi-modal masked autoencoders for medical vision-and-language pre-training. In *MICAI*, 2022.

[10] Navneet Dalal and Bill Triggs. Histograms of oriented gradients for human detection. In *CVPR*. IEEE, 2005.

[11] Alexey Dosovitskiy, Lucas Beyer, Alexander Kolesnikov, Dirk Weissenborn, Xiaohua Zhai, Thomas Unterthiner, Mostafa Dehghani, Matthias Minderer, Georg Heigold, Sylvain Gelly, et al. An image is worth 16x16 words: Transformers for image recognition at scale. In *ICLR*, 2021.

[12] Junying Gan, Shanlu Li, Yikui Zhai, and Chengyun Liu. 3d convolutional neural network based on face anti-spoofing. In *ICMIP*, 2017.

[13] Anjith George and Sébastien Marcel. Deep pixel-wise binary supervision for face presentation attack detection. In *ICB*, 2019.

[14] Anjith George and Sébastien Marcel. Learning one class representations for face presentation attack detection using multi-channel convolutional neural networks. *TIFS*, 2020.

[15] Anjith George and Sebastien Marcel. On the effectiveness of vision transformers for zero-shot face anti-spoofing. In *IJCB*, 2020.

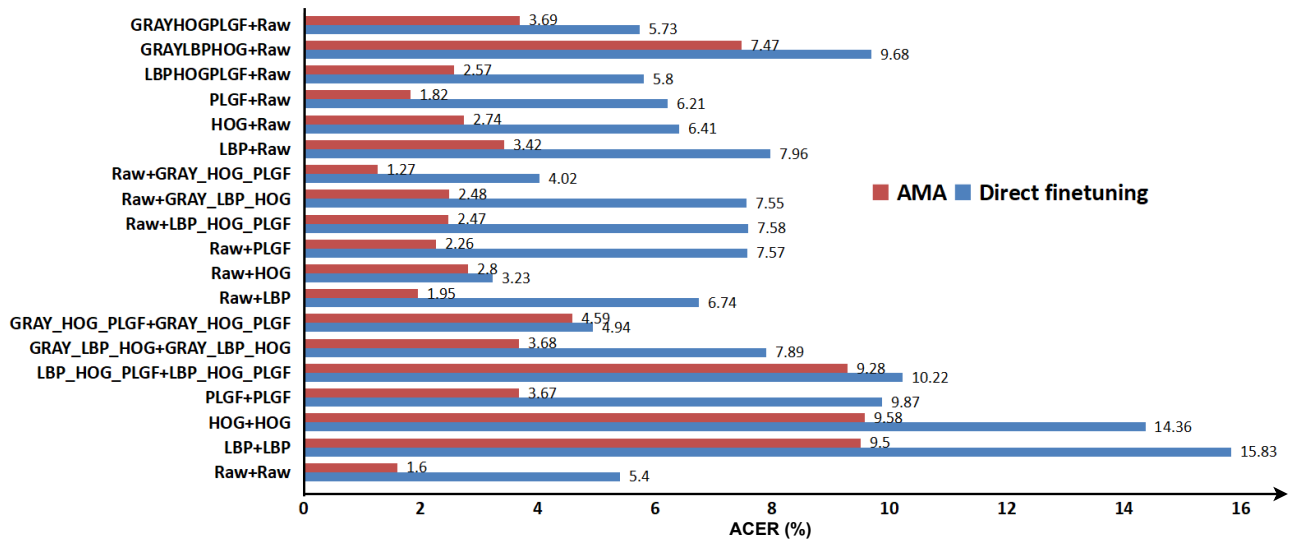
[16] Anjith George and Sebastien Marcel. Cross modal focal loss for rgbd face anti-spoofing. In *CVPR*, 2021.

[17] Anjith George, Zohreh Mostaani, David Geissenbuhler, Olegs Nikisins, André Anjos, and Sébastien Marcel. Biometric face presentation attack detection with multi-channel convolutional neural network. *TIFS*, 2019.

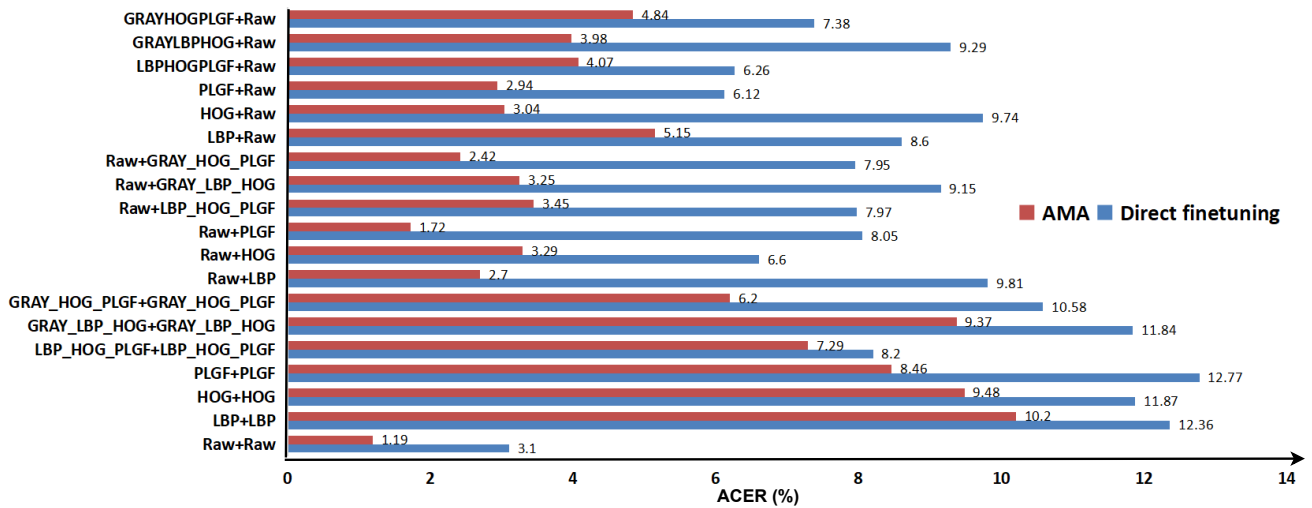
[18] Kaiming He, Xinlei Chen, Saining Xie, Yanghao Li, Piotr Dollár, and Ross Girshick. Masked autoencoders are scalable vision learners. In *CVPR*, 2022.

- [19] Neil Houlsby, Andrei Giurgiu, Stanislaw Jastrzebski, Bruna Morrone, Quentin De Laroussilhe, Andrea Gesmundo, Mona Attariyan, and Sylvain Gelly. Parameter-efficient transfer learning for nlp. In *ICML*, 2019.
- [20] Hsin-Ping Huang, Deqing Sun, Yaojie Liu, Wen-Sheng Chu, Taihong Xiao, Jinwei Yuan, Hartwig Adam, and Ming-Hsuan Yang. Adaptive transformers for robust few-shot cross-domain face anti-spoofing. In *ECCV*, 2022.
- [21] international organization for standardization. Iso/iec jtc 1/sc 37 biometrics: Information technology biometric presentation attack detection part 1: Framework. In <https://www.iso.org/obp/ui/iso>, 2016.
- [22] Shibo Jie and Zhi-Hong Deng. Convolutional bypasses are better vision transformer adapters. *arXiv preprint arXiv:2207.07039*, 2022.
- [23] Jukka Komulainen, Abdenour Hadid, and Matti Pietikainen. Context based face anti-spoofing. In *BTAS*, 2013.
- [24] Lei Li and Xiaoyi Feng. Face anti-spoofing via deep local binary pattern. In *Deep Learning in Object Detection and Recognition*, pages 91–111. Springer, 2019.
- [25] Zhi Li, Haoliang Li, Xin Luo, Yongjian Hu, Kwok-Yan Lam, and Alex C Kot. Asymmetric modality translation for face presentation attack detection. *IEEE TMM*, 2021.
- [26] Ajian Liu and Yanyan Liang. Ma-vit: Modality-agnostic vision transformers for face anti-spoofing. In *IJCAI*, 2022.
- [27] Ajian Liu, Zichang Tan, Jun Wan, Sergio Escalera, Guodong Guo, and Stan Z Li. Casia-surf cefa: A benchmark for multi-modal cross-ethnicity face anti-spoofing. In *WACV*, 2021.
- [28] Ajian Liu, Zichang Tan, Jun Wan, Yanyan Liang, Zhen Lei, Guodong Guo, and Stan Z Li. Face anti-spoofing via adversarial cross-modality translation. *TIFS*, 2021.
- [29] Ajian Liu, Chenxu Zhao, Zitong Yu, Jun Wan, Anyang Su, Xing Liu, Zichang Tan, Sergio Escalera, Junliang Xing, Yanyan Liang, et al. Contrastive context-aware learning for 3d high-fidelity mask face presentation attack detection. *TIFS*, 2022.
- [30] Weihua Liu, Xiaokang Wei, Tao Lei, Xingwu Wang, Hongying Meng, and Asoke K Nandi. Data fusion based two-stage cascade framework for multi-modality face anti-spoofing. *TCDS*, 2021.
- [31] Yaojie Liu, Amin Jourabloo, and Xiaoming Liu. Learning deep models for face anti-spoofing: Binary or auxiliary supervision. In *CVPR*, 2018.
- [32] Ilya Loshchilov and Frank Hutter. Decoupled weight decay regularization. In *ICLR*, 2017.
- [33] Zuheng Ming, Zitong Yu, Musab Al-Ghadi, Muriel Visani, Muhammad Muzzamil Luqman, and Jean-Christophe Burie. Vitranspad: Video transformer using convolution and self-attention for face presentation attack detection. In *ICIP*, 2022.
- [34] Usman Muhammad, Zitong Yu, and Jukka Komulainen. Self-supervised 2d face presentation attack detection via temporal sequence sampling. *Pattern Recognition Letters*, 2022.
- [35] Olegs Nikisins, Anjith George, and Sébastien Marcel. Domain adaptation in multi-channel autoencoder based features for robust face anti-spoofing. In *ICB*. IEEE, 2019.
- [36] Timo Ojala, Matti Pietikainen, and Topi Maenpaa. Multiresolution gray-scale and rotation invariant texture classification with local binary patterns. *IEEE TPAMI*, 2002.
- [37] Keyurkumar Patel, Hu Han, and Anil K Jain. Secure face unlock: Spoof detection on smartphones. *TIFS*, 2016.
- [38] Yunxiao Qin, Chenxu Zhao, Xiangyu Zhu, Zezheng Wang, Zitong Yu, Tianyu Fu, Feng Zhou, Jingping Shi, and Zhen Lei. Learning meta model for zero-and few-shot face anti-spoofing. In *AAAI*, 2020.
- [39] Tao Shen, Yuyu Huang, and Zhijun Tong. Facebagnet: Bag-of-local-features model for multi-modal face anti-spoofing. In *CVPRW*, 2019.
- [40] Ashish Vaswani, Noam Shazeer, Niki Parmar, Jakob Uszkoreit, Llion Jones, Aidan N Gomez, Łukasz Kaiser, and Illia Polosukhin. Attention is all you need. In *NIPS*, 2017.
- [41] Weihang Wang, Fei Wen, Haoyuan Zheng, Rendong Ying, and Peilin Liu. Conv-mlp: A convolution and mlp mixed model for multimodal face anti-spoofing. *IEEE TIFS*, 2022.
- [42] Zhuo Wang, Qiangchang Wang, Weihong Deng, and Guodong Guo. Face anti-spoofing using transformers with relation-aware mechanism. *IEEE TBIOIM*, 2022.
- [43] Zhuo Wang, Qiangchang Wang, Weihong Deng, and Guodong Guo. Learning multi-granularity temporal characteristics for face anti-spoofing. *IEEE TIFS*, 2022.
- [44] Tete Xiao, Mannat Singh, Eric Mintun, Trevor Darrell, Piotr Dollár, and Ross Girshick. Early convolutions help transformers see better. *NeurIPS*, 2021.
- [45] Xiao Yang, Wenhan Luo, Linchao Bao, Yuan Gao, Dihong Gong, Shibao Zheng, Zhifeng Li, and Wei Liu. Face anti-spoofing: Model matters, so does data. In *CVPR*, 2019.
- [46] Zitong Yu, Xiaobai Li, Xuesong Niu, Jingang Shi, and Guoying Zhao. Face anti-spoofing with human material perception. In *ECCV*, 2020.
- [47] Zitong Yu, Xiaobai Li, Pichao Wang, and Guoying Zhao. Transrppg: Remote photoplethysmography transformer for 3d mask face presentation attack detection. *IEEE SPL*, 2021.
- [48] Zitong Yu, Yunxiao Qin, Xiaobai Li, Zezheng Wang, Chenxu Zhao, Zhen Lei, and Guoying Zhao. Multi-modal face anti-spoofing based on central difference networks. In *CVPRW*, 2020.
- [49] Zitong Yu, Yunxiao Qin, Hengshuang Zhao, Xiaobai Li, and Guoying Zhao. Dual-cross central difference network for face anti-spoofing. In *IJCAI*, 2021.
- [50] Zitong Yu, Yuming Shen, Jingang Shi, Hengshuang Zhao, Philip HS Torr, and Guoying Zhao. Physformer: facial video-based physiological measurement with temporal difference transformer. In *CVPR*, 2022.
- [51] Zitong Yu, Chenxu Zhao, Zezheng Wang, Yunxiao Qin, Zhuo Su, Xiaobai Li, Feng Zhou, and Guoying Zhao. Searching central difference convolutional networks for face anti-spoofing. In *CVPR*, 2020.
- [52] Kevin Zhang and Zhiqiang Shen. i-mae: Are latent representations in masked autoencoders linearly separable? *arXiv preprint arXiv:2210.11470*, 2022.
- [53] Kaipeng Zhang, Zhanpeng Zhang, Zhifeng Li, and Yu Qiao. Joint face detection and alignment using multitask cascaded convolutional networks. *IEEE SPL*, 2016.

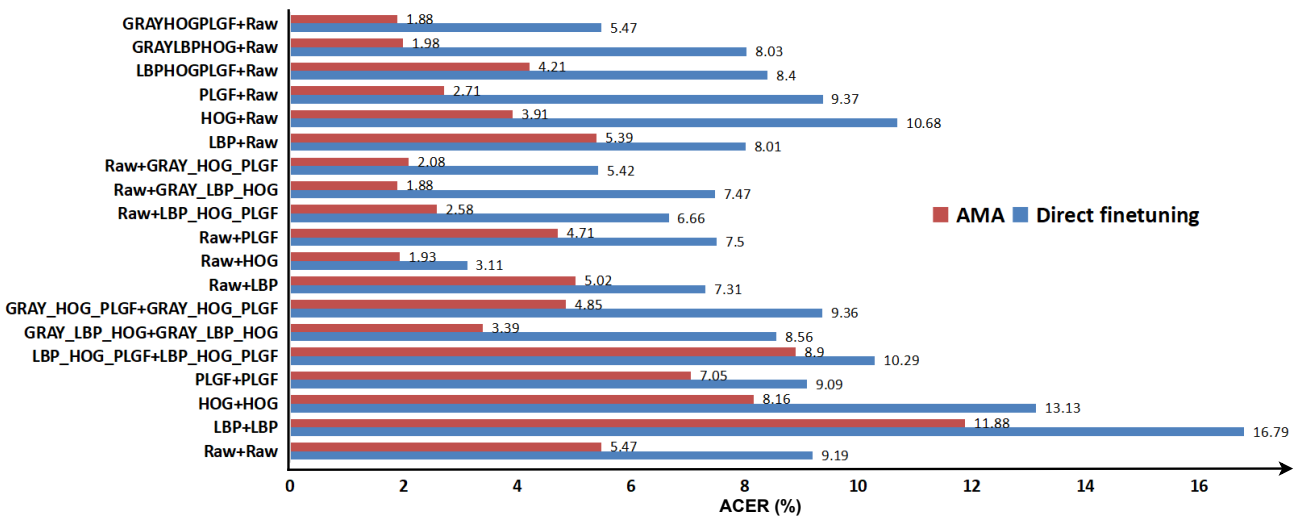
- [54] Peng Zhang, Fuhao Zou, Zhiwen Wu, Nengli Dai, Skarppness Mark, Michael Fu, Juan Zhao, and Kai Li. Feather-nets: Convolutional neural networks as light as feather for face anti-spoofing. In *CVPRW*, 2019.
- [55] Shifeng Zhang, Ajian Liu, Jun Wan, Yanyan Liang, Guodong Guo, Sergio Escalera, Hugo Jair Escalante, and Stan Z Li. Casia-surf: A large-scale multi-modal benchmark for face anti-spoofing. *TBIOM*, 2(2):182–193, 2020.
- [56] Shifeng Zhang, Xiaobo Wang, Ajian Liu, Chenxu Zhao, Jun Wan, Sergio Escalera, Hailin Shi, Zezheng Wang, and Stan Z Li. A dataset and benchmark for large-scale multi-modal face anti-spoofing. In *CVPR*, 2019.
- [57] Kaiyang Zhou, Jingkang Yang, Chen Change Loy, and Ziwei Liu. Learning to prompt for vision-language models. *IJCV*, 2022.



(a) RGB+IR modalities



(b) RGB+Depth modalities



(c) IR+Depth modalities

Figure 10. Impacts of bimodal inputs with local feature descriptors (e.g., LBP, HOG, PLGF) for ViT using direct finetuning and adaptive multimodal adapter (AMA) strategies on (a) RGB+IR; (b) RGB+Depth; and (c) IR+Depth modalities. ‘Raw+HOG’ indicates ‘Raw’ input and ‘HOG’ input are used for the first and second modalities, respectively.

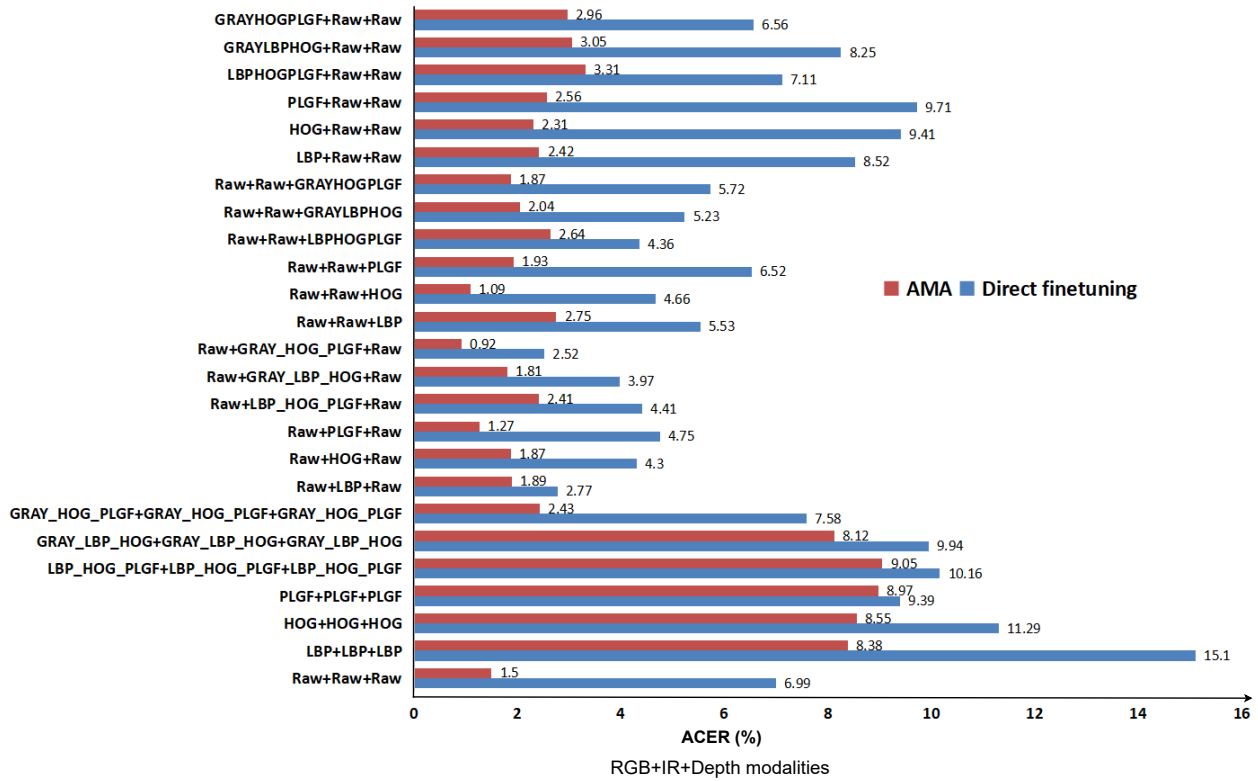


Figure 11. Impacts of trimodal inputs with local feature descriptors for ViT using direct finetuning and AMA strategies on RGB+IR+Depth modalities. ‘Raw+HOG+Raw’ indicates ‘Raw’ input, ‘HOG’ input and ‘Raw’ input are respectively used for three modalities.

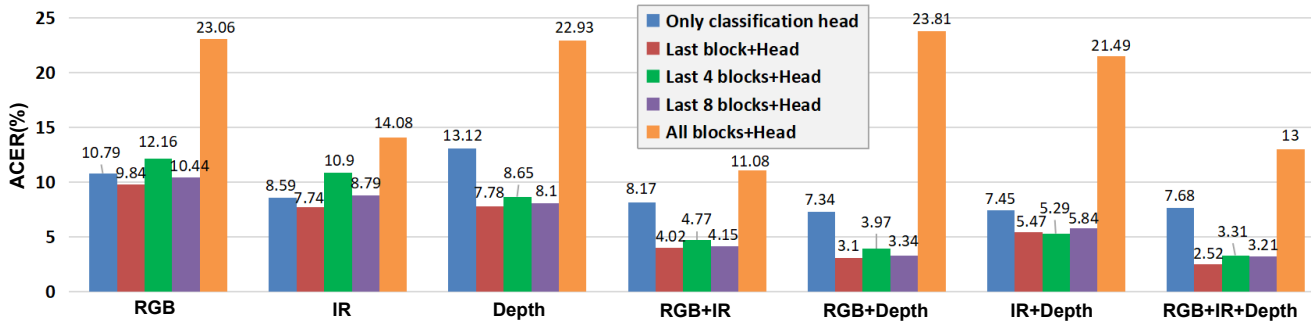


Figure 12. Results of direct finetuning on different transformer blocks.

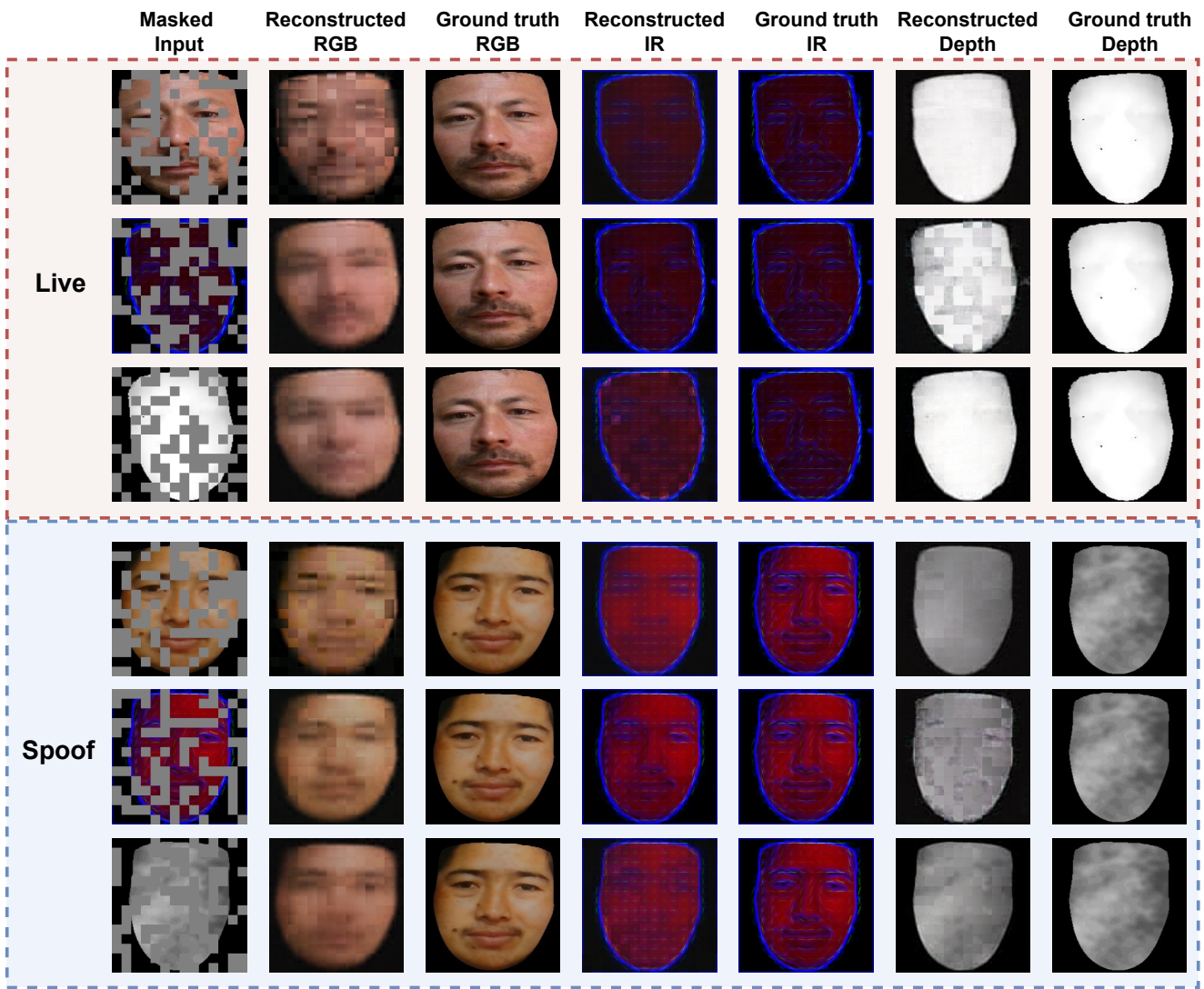


Figure 13. Visualization of the reconstructed multimodal faces from M^2A^2E with unimodal masked inputs on CeFA.